FORMATION AND PROPERTIES OF CELL-SIZE LIPID BILAYER VESICLES

P. MUELLER AND T. F. CHIEN
Department of Biochemistry and Biophysics, University of Pennsylvania, Philadelphia, Pennsylvania 19129

B. RUDY
Department of Physiology and Biophysics, New York University Medical Center, New York, New York 10016

ABSTRACT Hydration of single or mixed phospholipids or lipid protein mixtures at low ionic strength results in the formation of a population of large, solvent free, single bilayer vesicles with included volumes of up to 300 $\mu l/\mu mol$ lipid. Their size ranges from 0.1 to 300 μm and they can be sorted out according to size by centrifugation. When formed in distilled water their internal solution has a conductivity of 20–50 $\mu S/cm^{-1}$, an osmolarity of 0.5–5 mOsM, and a density of 1.0005–1.001. The osmotic pressure produced by the internal solutes cause a surface stress of 25 dyn/cm for a 20-μm vesicle. Their elastic constant ranges from 75–150 dyn/cm. During formation they can internalize particles such as latex beads or cell nuclei. They can be impaled with microelectrodes, or patch clamped. They can also be sealed to a small Vaseline-treated hole in a thin partition between two aqueous compartments. Sealing occurs in two stages. In the first stage sealing resistance is similar to that seen with patch-clamp pipettes. In the second stage, a much tighter seal is obtained. After sealing, the smaller portion of the sealed vesicle can be selectively broken by an electric shock leaving a single membrane across the hole. The capacitance and resistance of such membranes, in the presence of 10 mM NaCl, are $\sim$ 0.7 $\mu F/cm^2$ and 10^8 Ωcm^2 for pure lipid vesicles. Gramicidin increases the membrane conductance and monazomycin induces voltage-dependent gating thus providing further evidence that the vesicles are bounded by a single bilayer.

INTRODUCTION

Lipid bilayers large enough for direct electrical measurements have been a major tool in studying membrane phenomena (1). However, the methods currently available for their formation present certain technical shortcomings such as the retention of solvent in the bilayer or poor long-term stability. Furthermore, they are not available in bulk quantities and are thus unsuitable for chemical studies.

We report here on the formation and properties of solvent-free, large, cell-size lipid bilayer vesicles. They can be formed in bulk, have diameters of up to 300 μm, and can be studied by optical, chemical, and electrical techniques. They are stable for weeks and can also be formed from mixtures of protein and lipids. The technique for their formation is based on earlier observations by Reeves and Dowben (2), and Mueller and Rudin (3). A preliminary report was published elsewhere (4).

MATERIALS AND METHODS

Brain lipids were prepared from fresh bovine brains according to Mueller et al. (5). Asolectin, a mixture of phospholipids from soybean was obtained from Associated Concentrates and purified by the method of Kagawa and Racker (6). Various preparations of pure phosphatidylcholine, phosphatidylserine, and phosphatidylethanolamine were obtained from Supelco Inc. (Bellefonte, PA) or from Applied Sciences Laboratories, Gulf and Western Research and Development Group (Waltham, MA) and used without purification. Synthetic dipalmitoyllecithin was obtained from Applied Science Laboratories, Gulf and Western Research and Development Group, and cholesterol and tocopherol (DL-α) from Sigma Chemical Corp. (St. Louis, MO). Analytical grade reagents and double distilled and deionized water were used for all experiments. Gramicidin was obtained from Sigma Chemical Corp.

For the preparation of large vesicles phospholipids were water-washed by the following procedure. The lipids dissolved in $CHCl_3/CH_3OH$ 2:1 were emulsified with distilled water and the phases separated by low-speed centrifugation. The organic phase was extracted with water a total of 4 to 6 times. Lipids were stored in the dark as a 5–6° solution in chloroform under nitrogen at room temperature. The addition of deoxycholic acid or of tocopherol to the lipid solution before drying at a molar ratio of 100:1, lipid to additives, improves vesicle formation and does not interfere with the vesicle properties.

The density of the vesicles was determined by centrifugation on Ficoll or CsCl gradients. For analysis of their internal solution, the vesicles were concentrated by high-speed centrifugation and sonicated. The extravesicular volume was determined with radioactive glucose. Conductivity of the solutions was measured in a microchamber at 1 kHz and osmolarity was determined by freezing-point depression. The Na and K concentrations were obtained by flame photometry. Ionic fluxes across the vesicle membranes were studied by determining the internal radioactive tracer content after removing the external ions by ion exchange (7).

RESULTS

Formation of the Vesicles

Large vesicles form spontaneously when dried single phospholipids, phospholipid mixtures, or phospholipid-protein mixtures are hydrated at low ionic strength. Vesicles can be formed routinely from most single and mixed phospholipids. We have formed them from bovine brain lipid extracts, asolectin, purified egg-lecithin, synthetic dipalmitoyllecithin (DPL), phosphatidylserine, mixtures of these, and also in the presence of cholesterol or tocopherol. Better results are obtained after the synthetic lipids are extracted with water as described in the Methods section. In the case of DPL, vesicles form only above 40°C.

For the formation of the vesicles, 0.5 ml of a solution containing 5–6% lipid in chloroform or chloroform-methanol (2:1, vol/vol) is spread on the bottom of a 100-ml Erlenmeyer flask and dried completely under a stream of N_2. 100 ml of aqueous solution is added gently to the flask, which is then stored at 4°C. Shaking must be avoided. Vesicles appear as a white fluffy cloud at the bottom of the flask after 24–48 h. They can be prepared in distilled water, in solutions of nonelectrolytes such as glucose, sucrose, or Ficoll or in solutions of monovalent salts up to 10^{-4}M. The use of higher ionic strengths results in amorphous precipitates and myelin figures. Once formed, the vesicles are stable for weeks. The properties of the vesicles appear to be independent of the age of the preparation (up to 3 wk). The vesicles can be observed under phase contrast or bright field illumination in the presence of contrasting materials such as india ink or sonicated liposomes. However, the membranes are best visualized under dark field

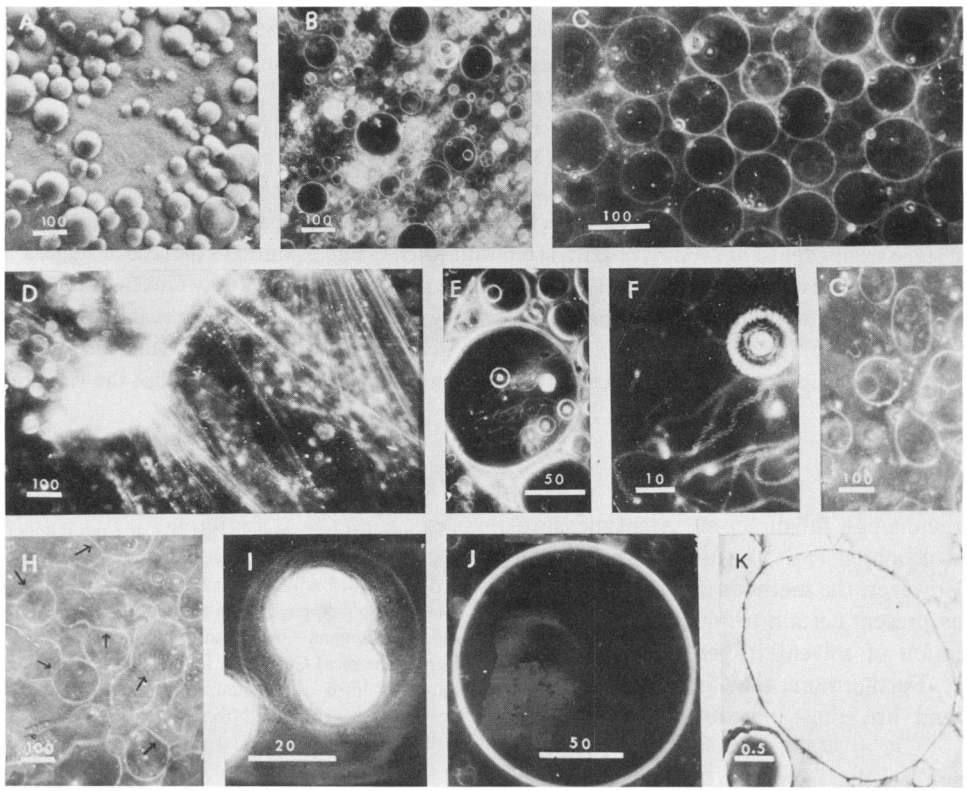

FIGURE 1 Micrograph of large lipid vesicles. (Calibrations in microns.) (*A*) Native preparation of bimolecular lipid vesicles observed under phase contrast. The contrast was enhanced by addition of sonicated liposomes. *(B)* Dark field image of a native preparation. Some of the vesicles appear white because they contain smaller vesicles and microtubules (see *D* and *F*). *(C)* A population of brain lipid vesicles prepared by centrifugation as described in Fig. 2. Some vesicles contain lipid microtubes. *(D)* Lipid microtubes extruded from broken large vesicles. The tubes are stretched by solvent flow due to evaporation at the cover-slip edge. *(E)* Vesicle containing strands of beaded tubes, clearly visible at higher magnification in *F*. *(G)* Vesicles that have lost water and have become flaccid after having been placed in 20 mM glucose for 5 min. *(H)* In the presence of 10 mM $CaCl_2$ the vesicles adhere to each other and form regions of close membrane contact *(arrows)*. *(I)* A vesicle containing two resin beads. When solid particles are present in the hydrating solution ~30% of the large vesicles contain such particles in their interior. In this way bacteria, cell nuclei, and red blood cells have been incorporated into the vesicles. *(J)* Single vesicle under dark field illumination. The relatively wide image of the membrane results from light reflected and scattered from a band of the internal membrane surface in the lower third of the vesicle. By raising the focus a second more narrow ring (not shown here) originating at a corresponding upper, outer circumference can be seen. When the vesicle is flaccid, Brownian motion of the membrane surface causes rapid fluctuations of the scattered light. *(K)* Electronmicrograph of a smaller vesicle. The vesicles were injected into warm agar fixed by glutaraldehyde and osmium permanganate and embedded and sectioned by standard methods. Micrograph obtained by J. Antanavage, Department of Biochemistry and Biophysics, University of Pennsylvania.

illumination. A summary of their optical appearance is shown in Fig. 1.

Aside from the large vesicles, the lipids also form long, thin tubes with diameters between 500 to 2,000 Å. Electronmicrographs show that the tube wall consists of a single lipid bilayer. Chains of very small vesicles joined by tubes are also seen (Fig. 1 *D–F*). These tubular structures are often contained inside the vesicles, but vesicles free of internal structures can be separated from those containing the tubes by centrifugation. The tubes contract into spheres in the presence of Ca^{++}.

The vesicles range in size from 0.1 to 300 μm (Fig. 2 *C*) and fractions of uniform diameters can be obtained by centrifugation in special tubes (see Fig. 2 *D* and *E*). When formed at 4°C, their average size grows over several days (Fig. 2 *F*) and included volumes of up to 300 μl/μmol of lipid have been observed. However, fusion between smaller vesicles has not been observed to take place during growth. During formation they can include neutral external solutes, e.g., sucrose and particles, such as latex beads up to 20 μm in diameter, present in the aqueous phase (Fig. 1 *I*).

When formed in distilled water, their internal solution has an average conductivity of 20 to 50 μS cm^{-1}, an osmolarity of ~2 mOsM, and a density of 1.0005–1.001. These densities are higher than those calculated from the lipid content of the vesicle membrane indicating the present of as yet unidentified internal solutes, perhaps lipid breakdown products and their counterions. Furthermore, the vesicles form smeared bands on Ficoll density gradients indicating inhomogeneities in the vesicle population.

The internal solutes cause an osmotic surface stress that for a 20-μm vesicle would amount to ~25 dyn/cm as calculated from the Laplace equation (see Discussion), and values between 0 and 20 dyn/cm are measured on vesicles of 80–100 μm by measuring the deformation of vesicles sucked to the end of a capillary under microscopic observation. By such measurements, the elastic constant for small changes of membrane area are found to be ~100 dyn/cm. Similar values were obtained by Kwok and Evans (8), who have calculated a value of 100 ergs/cm^2 at 25°C (or 0.5 kcal/mol of lecithin) for the reversible heat of expansion at constant temperature for the bilayer in these vesicles. When the osmotic gradient is reversed by adding external solutes, the vesicles become flaccid for short periods of time, but then they pinch off and regain a spherical shape. When flaccid, the vesicle's membrane fluctuates rapidly and the fluctuations can be observed under dark field by the light reflected from the membrane surface.

Electrical Properties

Initially the electrical properties of the vesicles were studied with microelectrodes as described in Fig. 3. A bridge circuit was used for these measurements. Penetration is signaled by a sudden bridge unbalance and an increase of the capacitance time constants. The membrane capacitance was estimated from these measurements as between

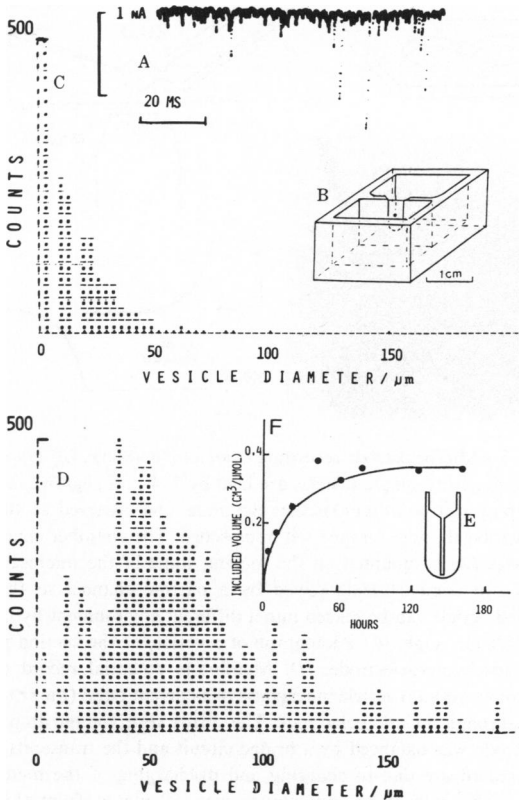

FIGURE 2 *(A–C)* Measurement of distribution of vesicle size. *(A)* Current transients observed when vesicles pass through a 200-μm apperture in a 10-μm thick Teflon partition, between the two compartments of the chamber shown in *B*. The two compartments contained 10^{-4}M Na aspartate, at a hydrostatic pressure difference of 3 mm and were held by voltage clamp at an electrical potential difference of 200 mV. As in a Coulter counter the amplitude of the current pulses is proportional to the vesicle volumes. *(C)* Vesicle diameter distribution of a 3-d old native sample. The distribution was obtained by computer analysis of the current transients shown in *A*. The computer program detected the peak amplitude and frequency for a 10-s flow sample and converted the data to diameter histograms as those shown in *C* and *D*. For a larger dynamic range the currents were fed into a logarithmic amplifier before storage and analysis. *(D–E)*. Separation of vesicles according to size. A small sample of vesicles (included volume ~50 μl) is diluted with the solution in which they were formed and spun in the special centrifuge tube shown in *E* at 40,000 *g* for 30 min in a swinging bucket rotor. The tube is made from polycarbonate and has a wide funnel-shaped opening at the top leading to a 6-cm long channel of 2-mm diam. For centrifugation, the diluted and dispersed vesicles were placed in the upper wide portion after the narrow portion had been filled with vesicle-free supernatant. The volume of the added vesicles should not exceed 3/4 of the volume of the narrow stem portion of the tube. During centrifugation the vesicles settled in the narrow stem portion of the tube according to size with the smaller vesicles at the bottom and the larger ones at the top. *D* shows the diameter distribution of the upper 20% of packed vesicles sedimented in the narrow stem of the tube, and corresponds in optical appearance to the vesicles shown in Fig. 1 *C*. *(F)* Increase of the specific vesicle volume during vesicle formation as a function of time. The volumes were determined by centrifuging in the special tube (*E*) a 2-ml sample after gently dispersing the vesicles in the entire flask volume. The values shown were corrected for extravesicular space, which was determined by radioactive glucose to be between 30 and 35% with a mean of 32%.

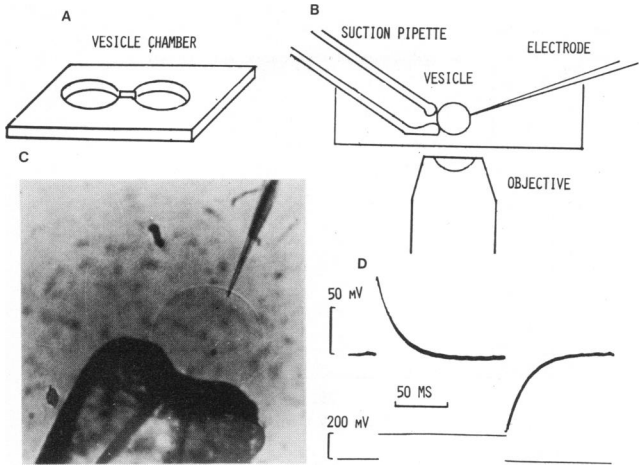

FIGURE 3 Microelectrode recording from a lipid vesicle. *(B)* For microelectrode puncture, single vesicles are held by 2–4-mm negative pressure at the tip of a 50-μm diam suction electrode, and observed at 400-fold magnification through an inverted microscope. The chamber containing the vesicles *(A)* is mounted on the moving stage of the microscope. It contains two compartments joined by a narrow channel so that the penetrated vesicle can be placed into a different environment by moving the microscope stage. *(C)* Photograph of a vesicle at the suction pipette with inserted microelectrode. *(D)* Membrane potential record (*upper* trace) from a 100-μm vesicle in response to a current pulse (*lower* record) injected through the microelectrode. The steady state voltage drop across the electrode was balanced by a bridge circuit and the transients in the voltage record are due to charging and discharging of the membrane capacity. The membrane capacitance was calculated from the time constant of the transient and the balancing resistance in the bridge as 0.7 μF/cm^2.

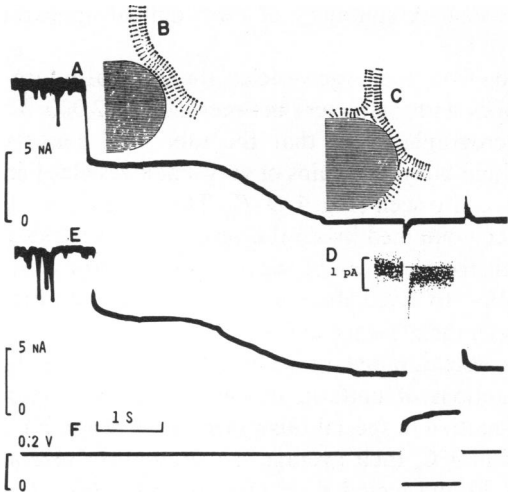

FIGURE 4 Sealing of a lipid vesicles on a hole in a Teflon partition. Vesicles flow under 3–4-mm hydrostatic pressure difference through a 70-μm hole in a thin Teflon partition separating the two aqueous compartments of the chamber shown in Fig. 2 *B*. The rim of the hole has been made hydrophobic by covering it with a 0.2% solution of Vaseline in pentane. The compartments are held by voltage clamp at a potential difference of 200 mV as indicated in *F*. A current vs. time record is shown in *A*. The current spikes at the beginning of the trace are caused by the passage of smaller vesicles through the hole as explained in Fig. 2. The current drops suddenly to a lower intermediate level as a vesicle that is larger than the hole sticks to the partition. This conductance is quantitatively similar per length of contact to seal resistances typically observed with patch-clamp electrodes (see Discussion). Subsequently, the current falls to almost zero because the vesicle membrane forms a tight seal with the partition. A transient reduction of the potential difference to zero (see *F*) leads only to capacitative transients but no steady current is observable at this gain. The diagrams *B* and *C* show how the conductance difference of the two sealing states might be explained by the bilayer configurations in contact with the hole's rim. In *B* the bilayer is intact and the apposition of polar lipid groups and rim material forms a conductive channel that accounts for the relatively large current during the first sealing stage. Subsequently, the bilayer forms a highly hydrophobic seal with the rim material, presumably by molecular rearrangement as shown in *C*. *(D)* At higher gain the residual current for a 200-mV pulse can be measured and, assuming that the seal conductance is negligibly small, the membrane conductance can be calculated from this value and the hole diameter, as explained in Fig. 5. Values range from between 1 to 2 $\times 10^{-8}\,\Omega^{-1}\text{cm}^{-2}$. *(E)* When 10^{-7}M gramicidin is added to the solution containing the vesicles, the two stage sealing process is still observed. However, the current does not fall to zero during the second stage, and a large current drop results when the clamp potential is reduced to zero. In this case, the membrane resistance was 2.6 $\times$ 10^4 Ωcm^2.

0.6 and 0.7 μF/cm^2; however, the membrane resistance could not be determined because of the incomplete seal of the microelectrode. Furthermore, microelectrodes do not allow for an easy change of the internal solution and their use is generally cumbersome. To obviate these problems we have developed methods in which the vesicle is sealed under gentle hydrostatic pressure to a hole in a thin partition between two compartments (Fig. 4).

The membrane conductance and capacitance can be measured without breaking the vesicle as shown in Fig. 5; however, to measure potentials across the membrane, or to control the membrane potential, a single membrane is required. This is achieved by breaking the smaller portion of the sealed membrane by an electrical shock leaving a single solvent-free bilayer membrane separating two aqeuous compartments (Fig. 6). The increase in the capacity (Fig. 6 *B*) suggests that indeed the small portion of the vesicle has been broken leaving a single membrane. The dielectric breakdown of the membrane drops from 400–500 mV for a whole sealed vesicle to ~200 mV after a portion of the vesicle is broken, and only under these conditions does monazomicin induce voltage-dependent conductances as it does in planar bilayer membranes. Stability of the single membranes varies between experiments, but we have obtained membranes lasting for 1–2 h routinely. The aqueous phase surrounding the membrane can be exchanged and high ionic strength solutions are tolerated. We have constructed a special chamber shown in Fig. 7 that restricts the aqueous phases to a few microliters and facilitates rapid and complete exchange of the aqueous solution on both sides without breaking the membrane.

Sealed vesicles or single membranes give similar values for the membrane capacitance and the membrane conductance. The range of values obtained from several hundred measurements is shown in Table I. The membrane capacitance is near that expected for a single bilayer membrane. The membrane resistance is ~10^8 Ωcm^2 and similar in value to that obtained with other pure lipid membranes

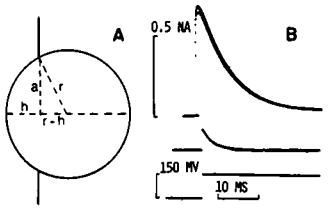

FIGURE 5 Method for determining the membrane resistance and capacitance. (*A*) Geometric relations for a vesicle sealed to a hole as in Fig. 4. When sealing is complete the capacitance and resistance measured with a voltage pulse applied across the partition is that of the two portions of the vesicle in series. The measured capacitance will be that of two capacitors in series, each with a specific capacitance C_O. The capacitance measured across the hole, C_v, with an intact vesicle sealed to the hole is the same as that for a single membrane of the same specific capacitance having an area equivalent to that of the hole.[1] The measured capacitance of the vesicle, C_v, is independent of vesicle size and equal to the capacitance, C_m, of a planar bilayer membrane across the hole. Similar relations hold for the resistance so that specific membrane resistance and capacitance can be measured without breaking the vesicle. (*B*) Four voltage-clamp capacity currents from four different vesicles sealed to the same aperature are superimposed. The four current records are identical even though the vesicles have different sizes. The *lower* trace shows the voltage applied across the partition and the vesicle, the *middle* trace, the capacity current of the partition without a vesicle. This is subtracted from the *upper* trace to calculate the membrane capacitance.

(9). The vesicles can also be patch clamped with the same techniques developed for single cells (10).

Permeability to Solutes

Although the electrical measurements indicate that the membrane is quite impermeable to ions, there is a discrepancy between the ionic permeability as measured by radioactive fluxes and that predicted from the electric conductivity of the membrane. The fluxes show two time constants, the first of which is on the order of minutes and the second several days. Observations with fluorescent solutes show that a fraction of the vesicles opens and closes

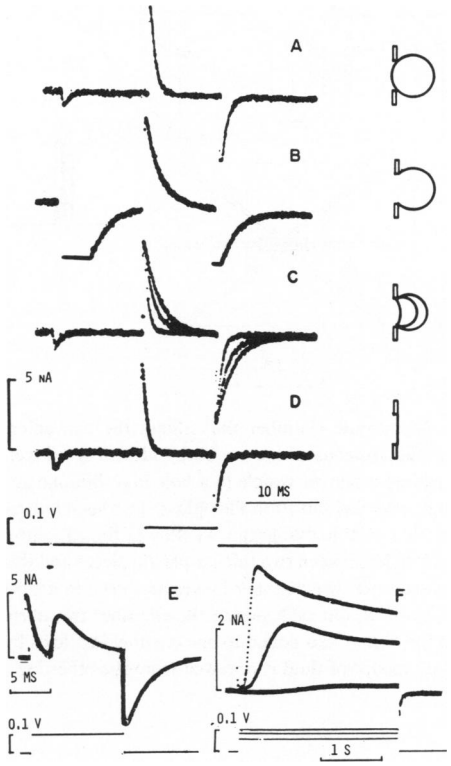

FIGURE 6 Breaking of one side of a vesicle sealed to a hole by an electric pulse. Two voltage pulses (shown below *D*) were applied in sequence after the vesicle sealed to the hole rim (see Fig. 4). In *A* the first pulse had an amplitude of 100 mV and a duration of 300 μs. The time integrals of the current transients generated by the second pulse are a measure of the capacity. In *B* the amplitude of the first pulse was raised to 1 V. This broke selectively the smaller portion of the vesicle membrane (see diagram to the right) because the voltage drop across the membrane is inversely proportional to the capacity and, therefore, larger than the voltage drop across the larger portion. The capacitative current caused by the breaking pulse is partially off screen. The currents for the second pulse have a longer time constant corresponding to the capacity of the remaining vesicle portion that is larger than that of the two portions in series (see Fig. 5). (*C*) Three superimposed current records taken after *B* at 1-min intervals. The amplitude of the first pulse was reduced to 10 mV. The time constants and integral of the capacity currents decrease with time, because the remaining vesicle membrane flattens out on the hole, as shown in the diagram. (*D*) The final steady state value taken 6 min after the breaking pulse shows a current integral only slightly smaller than that of the intact vesicle that was somewhat deformed due to the hydrostatic pressure difference. The single flat membrane is stable and solutions on both sides can be exchanged easily by using the chamber shown in Fig. 7. (*E*) Current trace during the breaking of one portion of the sealed vesicle. In this case, the membrane broke spontaneously during a 100-mV pulse. The sudden increase of the capacitance generated the second current transient. Notice that it is larger than the first transient at the start of the pulse and that the transient at the end of the pulse has a larger integral than the first because the membrane capacity has increased. (*F*) Membrane currents in response to applied potentials in the presence of 10^{-6}M monazomycin. The monazomycin was added after the small portion of the vesicle was broken and the membrane had become flat. Such voltage dependent currents are only observed in single bilayer membranes and not in intact vesicles. This further demonstrates that there is a single bilayer across the hole.

[1]Fig. 5 is governed by the following equations. The area of the membrane on one side is $2\pi rh$, that on the other side has an area equal to $2\pi r(2r - h)$. Thus the capacitance across the hole is

$$C_v = \frac{1}{\frac{1}{C_o 2\pi rh} + \frac{1}{C_o 2\pi r\,(2r - h)}} = C_o\pi(2rh - h^2). \quad (1)$$

The capacitance of a hypothetical membrane (C_m) with an area equal to that of the hole (πa^2) and with the same specific capacitance as that of the vesicle (C_o) would be

$$C_m = C_o\pi a^2 \quad (2)$$

where

$$a = \sqrt{r^2 - (r - h)^2}\,. \quad (3)$$

Therefore

$$C_m = C_o\pi[r^2 - (r - h)^2] = C_o\pi(2rh - h^2) = C_v. \quad (4)$$

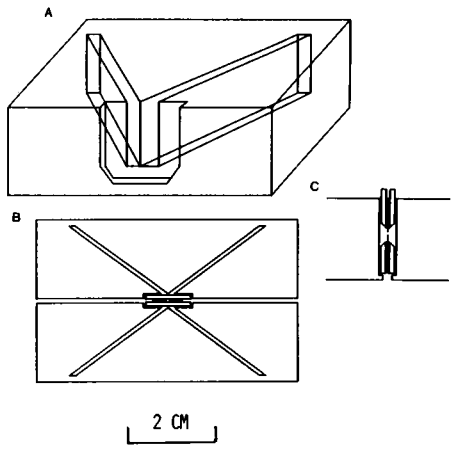

FIGURE 7 Membrane chamber that allows the convenient and rapid exchange of the aqueous phase on both sides of a bilayer membrane formed by sealing a bilayer vesicle to a hole in a thin plastic partition. *A* shows one half chamber cut from Plexiglass. Two such half chambers are clamped together. A thin diaphragm (Teflon or Saran) with a small hole in the center is held between two thicker plastic pieces and the assembly is clamped between the two chamber halves as shown in cross section in *C* and in top view in *B*. On each side of the chamber two narrow channels converge on the hole. Fluid added to one channel leg flows by the hole as an equivalent amount of fluid is removed from the other leg. Scale refers to *B*.

TABLE I
PROPERTIES OF CELL-SIZE BILAYER VESICLES

Properties of bilayer vesicles	Mean	Range
Population properties		
Diameter	5 μM	0.1–300
Internal volume (per milligram lipid)	0.2 cm^3	0.15–0.3
Density	1.00075	1.0005–1.001
Properties of internal solution*		
Conductivity	25 $\mu S\ cm^{-1}$	20–50
Osmolarity	2 mOsM	0.5–5
Osmotic pressure	6×10^4 dynes cm^{-2}	—
$[Na^+]$	$<10^{-4}$ M	—
$[K^+]$	1.1×10^{-4} M	—
pH	6.4	—
Mechanical membrane properties		
Surface stress	7 dynes cm^{-1}	0–20
Elastic constant	100 dynes cm^{-1}	75–150
Electrical membrane properties		
Capacitance	0.6 $\mu F\ cm^2$	0.55–0.7
Dielectric thickness	25Å	—
Dielectric strength	220 mV	200–300
Membrane permeability		
Na^+ (permeability coefficient)	2.5×10^{-11} cm s^{-1}	—

*For vesicles prepared in distilled water: ([Na], [K], $<10^{-5}$ M, conductivity 0.2 $\mu S\ cm^{-1}$, osmolarity <0.1 mOsM, pH 6.8).

transiently. When vesicles are suspended in a solution containing carboxyfluorescein some vesicles open and include the fluorescent dye in their interior. The entrance of the dye occurs within seconds, but individual vesicles stain at different times during the observation suggesting that it is not a membrane permeation of the dye. Furthermore, on some ocassions, the vesicles can actually be seen to open and reclose. This phenomenon also allows for the loading of vesicles by dialysis with ions and other solutes after they are formed provided that the osmotic gradient is kept close to zero.

Preparation of Protein-containing Vesicles

Proteins can be inserted into the vesicles, either before, during, or after the vesicle formation. In the first case, small liposomes are reconstituted with the membrane proteins. Ions are removed from the liposomes by dialysis. The liposomes are then lyophilized after addition of glucose and rehydrated with water. This method has worked well for cytochrome oxidase. The resulting large vesicles showed respiratory control. The rate of oxidation of external cytochrome *c* by reconstituted vesicles resuspended in 10 mM KCl was accelerated 1.7–2 times upon addition of gramicidin or valinomycin and nigericin indicating the functional integrity and membrane incorporation of the oxidase.

As an alternative procedure, the membrane proteins can be added to the hydrating solution and thus be present during vesicle formation. Low concentrations of detergents that are tolerated during formation are helpful. The proteins may also be added from their detergent solution to preformed vesicles. The vesicles tolerate up to 1% cholate for short periods of time. Darzon et al. (11) have formed vesicles through hydration of lipid-protein complexes dried from apolar solvents. Perhaps the most gentle procedure would be the incorporation of native membrane fragments or reconstituted liposomes into preformed vesicles by fusion. However, this approach has not yet been investigated.

DISCUSSION

Most of the vesicles are bounded by a single bilayer. This is evident from the values of membrane capacitance and the dielectric breakdown potential, which are within the range expected for a single bilayer. In addition, gramicidin (Fig. 4) and monazomicin (Fig. 6), known to form channels only in single bilayers (12), show the same activity in the vesicle membranes. Multilayer membranes can be distinguished optically because under conditions of low ionic strength the individual layers separate and are clearly visible. Little is known about the process by which these structures form. Visual observations indicate that single bilayer blisters can separate from a multilayer or gel phase and subsequently pinch off into vesicles. However, the slow growth of the vesicle population indicates that other mechanisms, including fusion, may be involved.

The vesicle surface is apparently under tension. The vesicles are perfectly round and when they are broken with a microelectrode, water flushes out rapidly and the vesicle contracts and moves in the opposite direction. The internal pressure (p) maintaining the vesicles under tension is probably of osmotic origin satisfying the Laplace equation $p = 2\gamma/r$, where γ is the surface stress, and r the vesicle radius. The measured osmolarity of the internal solution of ~2 mOsM would generate a pressure of 0.5×10^5 dyn/cm^2 and a surface stress of ~25 dyn/cm for a vesicle having a diameter of 20 μm. Internal solutes, probably lipid breakdown products and their counterions, are most probably responsible for the osmotic pressure, which may vary with vesicle size.

As shown in Fig. 4, the sealing of the vesicle membrane to a Vaseline-pretreated hole is a two stage process. In the first stage the vesicle makes only a relatively low resistance contact, which has an average value of 10^6 Ω/cm of linear contact. At low ionic strength, the specific conductance of the contact region is much higher than that of the bulk solution, presumably, because the fixed charges of the lipid surface provide a high concentration of mobile counterions. As a result, the current seen in Fig. 4 drops only by one third, when the entire hole is obstructed by the vesicle. Note that the above value of 10^6 Ωcm^{-1} should predict a seal resistance of 10^{10} Ω for a bilayer attached to the tip of a 0.3-μm diam micropipette, a value typically observed with patch-clamp pipettes (10).

On the other hand, the second sealing stage that develops subsequently has a much higher linear resistance, of more than 2×10^{10} Ωcm^{-1}. We argue that this tight seal results from hydrophobic interaction of the lipid tails with the Vaseline coating. This high seal resistance may be advantageous for electrical measurements of membranes that have a high inherent resistance. The vesicles may be useful for studies of membrane reconstruction and investigation of physical properties of lipid bilayers. For example, Wolf et al. (13) have applied fluorescence photobleaching recovery to study the diffusion of molecules in the plane of the membrane of such vesicles. They found that stearoyl dextrans diffuse at room temperature with a diffusion coefficient $D = 2 \times 10^{-9}$ cm^2/s, ~2 to 3 times slower than in solvent containing black lipid films. Large vesicles can also be formed by fusing small phospholipid or phospholipid-protein vesicles by freeze-thaw (14). These vesicles can be formed in high ionic strength solutions. However, the yield of unilamellar vesicles is far less and the maximal size of these vesicles is typically 5 to 10 μm and thus much smaller than those obtained by the method described here.

The technical assistance of J. Antanavage, Y. C. Ching, and L. Dunlap is greatly appreciated. We also thank Dr. R. Bartkowsky and W. Singer for stimulating discussions.

This research was supported in part by grant GM 25256 to P. Mueller and GM 26976 to B. Rudy.

Received for publication 20 July 1983 and in final form 30 August 1983.

REFERENCES

1. Miller, C., and C. Racker. 1979. Reconstitution of membrane transport functions. *In* The Receptors. R. D. O'Brien, editor. Plenum Press, New York. 1:1–31.
2. Reeves, J. P., and R. M. Dowben. 1969. Preparation and properties of thin-walled phospholipid vesicles. *J. Cell. Physiol.* 73:49–60.
3. Mueller, P., and D. O. Rudin. 1968. Resting and action potentials in experimental bimolecular lipid membranes. *J. Theoret. Biol.* 18:222–258.
4. Antanavage, J., T. F. Chien, Y. C. Ching, L. Dunlap, P. Mueller, and B. Rudy. 1978. Formation and properties of cell-size single bilayer vesicles. *Biophys. J.* 21(2, Pt. 2):122*a. (Abstr.)*
5. Mueller, P., D. O. Rudin, H. T. Tien, and W. C. Wescott. 1962. Reconstitution of cell membrane structure and its transformation into an excitable system. *Nature (Lond.).* 194:979–980.
6. Kagawa, Y., and E. Racker. 1971. Partial resolution of the enzymes catalyzing oxidative phosphorylation. XXV. Reconstitution of particles catalyzing ^{32}Pi-adenosine triphosphate exchange. *J. Biol. Chem.* 246:5477–5487.
7. Gazco, O. D., A. F. Knowles, H. G. Shertzer, E. Suolina, and E. Racker. 1976. The use of ion-exchange resins for studying ion transport in biological systems. *Anal. Biochem.* 72:57–65
8. Kwok, R., and E. Evans. 1981. Thermoelasticity of large lecithin bilayer vesicles. *Biophys. J.* 35:637–652.
9. Montal, M., and P. Mueller. 1972. Formation of bimolecular membranes from lipid monolayers and a study of their electrical properties. *Proc. Natl. Acad. Sci. USA.* 69:3561–3566.
10. Hamill, O.P., A. Marty, B. Neher, B. Sakman, and F. J. Sigworth, 1981. Improved patch-clamp techniques for high resolution current recording from cells and cell-free membrane patches. *Pfluegers Arch. Eur. J. Physiol.* 391:85–100.
11. Darzon, A., C. A. Vandenberg, M. Schoenfeld, M. H. Ellisman, N. Spitzer, and M. Montal. 1980. Reassembly of protein-lipid complexes into large bilayer vesicles: perspectives for membrane reconstitution. *Proc. Natl. Acad. Sci. USA.* 77:239–243.
12. Mueller, P. 1979. The mechanism of electrical excitation in lipid bilayers and cell membranes. *In* The Neurosciences: Fourth Study Program. F. O. Schmitt and F. G. Warden, editors. MIT Press, Cambridge, MA. 641–658.
13. Wolf, D. E., P. Henkart, and W. W. Webb. 1980. Diffusion, patching and capping of stearoylated dextrans on 3T3 cell plasma membranes. *Biochemistry.* 19:3893–3904.
14. Kasahara, M., and P. C. Hinkle. 1977. Reconstruction and purification of the d-glucose transport protein from human erythrocytes. *In* Biochemistry of Membrane Transport. G. Semenza and E. Carafoli, editors. Springer-Verlag New York, Inc., New York. 346–350.